orebodies and in mineralized veins led us to draw certain conclusions and deduce a series of genetic implications.

(1) The results obtained on the fine structure of aureoles of Pb, Zn, and Cu distribution developing in the wall-rock granite around veins indicates that they can be used to reconstruct elements of rock-water interactions in the ore-forming hydrothermal system and propose a scheme of a model for the genesis of the ore and aureoles.

(2) The region where a variety of elements (including ore elements and sulfide sulfur) are mobilized can be spatially restricted to the junction zone between a regional fault and its splay shear and detachment fractures, in which vein orebodies develop.

(3) The deposits studied within the scope of this research are dominated by aureoles whose maxima of metal concentrations are shifted away from the vein selvages for different distances (aureoles of type B). There are no aureoles whose Zn, Pb, and Cu distributions are close to the exponential law alone (type A). The dominance of type-B distributions suggests that ore formation was associated with a change from metalliferous to barren solutions (at least in terms of any one metal or even all of them).

(4) The switch from metalliferous to barren solutions could occur more than once over the mineral stage during the evolution of the hydrothermal system. The decrease in the concentrations of Zn, Pb, and Cu or the barren character of the fluid in terms of these components occurred asynchronously for all metals. The weak correlations between the distributions of the metals in veins and aureoles and the dominance of Zn in the aureoles led us to propose that the Zn concentration in the metalliferous mineralized solution was higher than the Pb and Cu concentrations.

(5) The probable mechanisms responsible for the origin of the primary aureoles at vein deposits were deposition, redeposition, and leaching.

(6) We have demonstrated that in aureoles, ore elements are mostly redeposited and accumulated (the only exception is leaching aureoles), while in veins ore elements can be partly or fully dissolved and redeposited along the general vector of fluid movement in the fracture conduit.

(7) The totality of geochemical data led us to propose elements for the genetic model of ore formation and the development of aureoles. These elements comprise, first of all, a probable scheme of fluid filtration flows in the ore-forming hydrothermal system.

CHAPTER 6
EQUILIBRIUM–DYNAMIC MODELS FOR THE MOBILIZATION OF ORE COMPONENTS AND THE DEVELOPMENT OF ORE MINERALIZATION AND ALTERATION AUREOLES AT VEIN BASE-METAL DEPOSITS

Based on the geological model that is underlain by the results of geochemical studies at Pb–Zn deposits (see Chapter 5), let us now consider equilibrium–dynamic models for the main elements of the ore-forming system: regions where metals are mobilized, where metals are transported and veins develop, and where aureoles develop.

As before, our methodological approach involves the analysis of models for the genesis and evolution of the hydrothermal systems (from the region where the ore material is mobilized to the regions where ore mineralization is formed and aureoles grow) as a chain of an interrelated and self-adjusting sequence of events [Borisov and Goreva, 1994, 1995a; Borisov *et al.*, 1995b; Borisov and Shvarov, 1995, 1996, 1998; Borisov and Kudryavtsev, 1996, 1999; Borisov *et al.*, 1997, 2002; Borisov, 2000a, 2000b, 2000c].

6.1. Model for the Mobilization of Ore Components

One of the very first stages in simulating ore-forming processes is the specification (or determination) of the load of ore components of the probable initial hydrothermal fluid. Inasmuch as it was established (see the results listed in Chapter 5) that a possible source of ore components can be the host granite, the main task of the first phase of simulations is to test this possibility and identify the principal factors that control the mobilization of metals from a natural granite. For this purpose, we examined a series of models for the mobilization of ore components over broad ranges of temperature, pressure, and the composition of the primary (barren) hydrothermal solution.

6.1.1. Model formulation and simulation techniques

Let us recall (based mainly on literature data) the main thermodynamic parameters of the hydrothermal system that can be used to specify our simulation conditions and parameters.

(1) Temperature generally varies over the interval of 415–65°C (the quartz–galena–sphalerite ore stage spans a range of 345–120°C) [Laz'ko *et al.*, 1981; Lyakhov *et al.*, 1994]. The paleodepth at which the deposits were formed corresponded to 2.5–3.0 km [Nekrasov, 1980]. The temperature of the country rocks during ore formation could be 100–150°C (at a temperature gradient of 35–50°C/km). Our models deal with mobilization processes at different temperatures, but the basic leaching model was assumed to operate at 370°C (i.e., 25°C higher than the maximum for the quartz–galena–sphalerite ore stage).

Table 35. Average compositions of granite from the Kholst and Verkhnii Zgid deposits [Gotman and Malakhov, 1966] and their recalculation to atomic amounts of the elements per 1 kg of the rock*

Granite from the Kholst deposit				Granite from the Verkhnii Zgid deposit			
oxide	wt %	element	gram atom/kg of rock	oxide	wt %	element	gram atom/kg of rock
SiO_2	71.75	Si	11.94	SiO_2	72.75	Si	12.11
Al_2O_3	13.98	Al	2.74	Al_2O_3	13.28	Al	2.6
Fe_2O_3	0.105	Fe	0.33	Fe_2O_3	0.31	Fe	0.257
FeO	2.333	Mg	0.16	FeO	1.34	Mg	0.11
Fe_S^{**}	0.0525	Ca	0.17	Fe_S^{**}	0.15	Ca	0.18
MgO	0.66	Na	0.96	MgO	0.44	Na	0.92
CaO	0.96	K	1.06	CaO	1.04	K	1.14
Na_2O	3.0	H	1.8	Na_2O	2.88	H	2.0
K_2O	4.965	O	30.559	K_2O	5.37	O	30.691
H_2O	1.612	S	0.016	H_2O	1.8	S	0.054
S	0.06	Zn	0.0005	S	0.17	Zn	0.0005
		Pb	0.0002			Pb	0.0002
		Cu	0.0003			Cu	0.0003

*MnO, TiO_2, and P_2O_5 (<0.5 wt % in sum) were excluded from the analysis and further consideration. LOI was considered to be caused by H_2O loss. Ore components (Zn, Pb, and Cu) were introduced into the system in the form of oxides.
**All Fe ascribed to pyrite.

(2) The overall pressure interval is 2.3–0.1 kbar. A pressure close to the lithostatic value at the aforementioned paleodepth should have been equal to 0.8–1.0 kbar. Our models deal with mobilization processes under different pressures, but most calculations were conducted for $P = 1$ kbar.

(3) Numerous analyses of gas–liquid inclusions [Lyakhov *et al.*, 1978, 1994] suggest that the fluids were rich in chlorides and carbonates (>50% chlorides). The probable proportions of major components in the primary hydrothermal solution was borrowed from [Lyakhov *et al.*, 1978]. Our models deal with primary hydrothermal solutions with different proportions of major components.

The average compositions of the presumably unaltered granites from the Kholst and V. Zgid deposits are reported in Table 35, which also presents the recalculations of the analyses of atomic quantities of elements (which were used to specify the bulk composition of the system for thermodynamic calculations). The background concentrations of ore elements in the granites were determined as follows (wt %): Zn = 0.004, Pb = 0.003, and Cu = 0.002 (when recalculated to gram atoms per 1 kg of the rock, these are Zn = 0.0005, Pb = 0.0002, and Cu = 0.0003).

The thermodynamic calculations were conducted using the GBFLOW computer program (a modification of the GIBBS program) and the HCh program package [Shvarov, 1992, 1999; Shvarov and Bastarkov, 1999]. The granite–fluid system was described by 15 independent components: H, O, K, Na, Ca, Mg, Al, Fe, Si, C, Cl, S, Zn, Pb, and Cu. The model aqueous fluid included 79 species, among which 26 species were of ore elements: Cu^+, $CuOH^0$, $Cu(HS)_2^-$, $Cu(HS)_2H_2S^-$, $CuOHCl^-$, $CuCl^0$, $CuCl_2^-$, $CuCl_3^{2-}$, Cu^{2+}, Zn^{2+}, $ZnOH^+$, $Zn(OH)_2^0$, $ZnHCO_3^+$, $Zn(HS)_2^0$, $ZnCl^+$, $ZnCl_2^0$, $ZnCl_3^-$, $ZnCl_4^{2-}$, $ZnSO_4^0$, Pb^{2+}, $PbOH^+$, $Pb(HS)_2^0$, $PbCl^+$, $PbCl_2^0$, $PbCl_3^-$, and $PbCl_4^{2-}$. The possible solid phases included 52 minerals (main rock-forming, metasomatic, and ore minerals). Thermodynamic data were calculated using the UNITHERM database for temperatures of 100–440°C and pressures from the saturated water vapor pressure to 1 kbar.

The mobilization zone of ore components (root zone of the hydrothermal system) was represented by a reactor with a specified constant amount of unaltered granite (most often, 10 kg), which contained background concentrations of Zn, Pb, and Cu (Table 35). A certain amount of the primary barren fluid (usually 1 kg of H_2O with dissolved salts) entered into the reactor and reacted with the granite. The rock was altered, and the newly formed solution in equilibrium with it was regarded to be the initial solution for the hydrothermal system in question (Fig. 50). The mobilization model is designed as the passage of several portions (waves) of

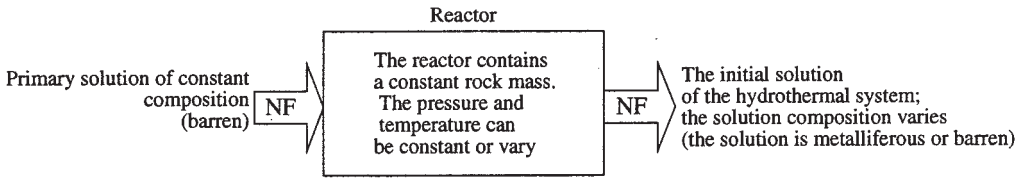

Fig. 50. Scheme for calculating the composition of the initial metalliferous solution. Arrows indicate the direction of solution flow (NF is the number of solution waves or flows coming into or going out the reactor).

the primary solution of constant composition through the reactor. In this variant of the model, the number of primary solution portions (waves, flows) can be regarded as a relative time scale. The thermodynamic calculations were conducted both for a constant temperature and pressure in the reactor and for varying values of them at different rock amounts and the compositions of the primary solution.

6.1.2. Thermodynamic simulation results

The calculation results are divided into six series.

1. Basic leaching model (IS-2). The model is regarded as provisionally basic, only because the maximum amount of calculation was conducted with the parameters used in this model.

Simulation conditions and parameters were as follows: T = 370°C, P = 1 kbar (which roughly corresponds to the lithostatic pressure), the granite mass in the reactor was equal to 10 kg (Kholst granite) and the water amount in a unit portion (wave) of the primary solution was 1 kg; i.e., the starting rock/water ratio was equal to 10 (R/W = 10). The salt composition of this solutions was 0.5 *m* H_2CO_3, 1.0 *m* NaCl, and 0.1 *m* HCl. The reactor was successively passed by 30 portions (up to 100 portions when necessary) or waves of the primary solution, because of which the integral rock/water ratio was changed to 0.33 or log R/W = –0.5.

Table 36 (data for waves 1, 10, 20, and 30) and Fig. 51 depict the results of the calculations for two reaction products: the leaching solution (Figs. 51a–51c) and altered rock (Figs. 51d–51f).[15] Plotted on the abscissa of all diagrams of Fig. 51 are the successive portions or waves (NF) of the primary solution.

The main characteristics of the leaching solution are manifested already in the first interaction wave (Table 36). Here the solution contains K (0.2 *m*), Ca (0.0098 *m*), Mg (1.9×10^{-5} *m*), Al (4.2×10^{-5} *m*), Si (0.0223 *m*), and Fe (0.0045 *m*). Its pH becomes nearly neutral (5.324), and the Na concentration decreases from 1 to 0.88 *m*. The concentrations of ore components are relatively high: 1.81×10^{-4} *m* Zn, 1.68×10^{-5} *m* Pb, 1.27×10^{-5} *m* Cu, and 2.16×10^{-2} *m* S.

As more and more new portions of the primary solution participate in the reaction, the system undergoes transformations associated with a systematic increase in the concentrations of ore components in the leaching solution: by a factor of 11 for Zn (from 1.8×10^{-4} *m* at wave 1 to 2×10^{-3} at wave 9), by a factor of 12 for Pb (from 1.7×10^{-5} *m* at wave 1 to 2×10^{-4} *m* at waves 13 and 19), and by a factor of 22 for Cu (from 1.3×10^{-5} *m* at wave 1 to 2.9×10^{-4} *m* at waves 13–19). The Cu concentration at waves 13–19 increases by a factor of 120 as compared to waves 2–6 (Fig. 51a). Simultaneously with the increase in the concentrations of the ore components, the concentration of sulfide sulfur decreases from 2.2×10^{-2} *m* at wave 1 to 3.4×10^{-4} *m* at wave 19, i.e., by a factor of 65.

As can be seen from Figs. 51a–51c, components are leached unevenly in discrete waves. For example, Zn passes into solution almost equally in each of the first six waves: 4% of the total metal concentration in granite for each wave, with the overall passage to the solution amounting to 23.7% (Figs. 51b, 51c). The intensity of Zn extracting drastically increases after wave 6 and becomes as high as 6% in NF = 7, 19% in NF = 8, 40% in NF = 9. At wave 10, Zn is extracted completely from the rock, so that the percentage of its passage into solution does not correspond anymore to the potential mobilizing ability of the primary solution (12% in NF = 10 is all Zn contained in the rock).

Pb and Cu are extracted less intensely but show analogous tendencies: low percentage of their passage into the equilibrium solution in the first six waves (~0.9% of Pb in each wave and ~0.1% of Cu), after which their leaching is intensified. Figure 51b demonstrates that Pb is extracted more actively than Cu in the first ten waves (12.56% of Pb and 10.65% of Cu are the integral figures for NF from 1 to 10), then both elements are leached equally, and the complete leaching of these metals and sulfide sulfur is attained simultaneously at wave 20. The sulfide sulfur concentration in the equilibrium solution becomes lower than the sum of the Pb and Cu concentrations (in NF = 19: 1.98×10^{-4} *m* Pb, 2.88×10^{-4} *m* Cu, and 3.42×10^{-4} *m* S). The sulfide sulfur content is higher than the concentrations of all ore metals only in NF = 1–13.

[15] In Fig. 51 and below in the text, the following notation is used: *Po*—pyrrhotite (FeS), *Py*—pyrite (FeS_2), *PbS*—galena, *ZnS*— sphalerite, *Cc*—chalcocite (Cu_2S), *Bn*—bornite (Cu_5FeS_4), *Ccp*— chalcopyrite ($CuFeS_2$), *Ep*— epidote ($Ca_2FeAl_2Si_3O_{13}H$), *Ep60*— epidote ($Ca_2Fe_{0.6}Al_{2.4}Si_3O_{13}H$), *Ep75*—epidote ($Ca_2Fe_{0.75}Al_{2.25}Si_3O_{13}H$), *Act*—actinolite ($Ca_2FeMg_4Si_8O_{24}H_2$, *Chl*$_{75}$—chlorite ($Mg_{1.25}Fe_3Al_{3.5}Si_{2.25}O_{18}H_8$), *Chl50*—chlorite ($Mg_{2.5}Fe_2Al_3Si_{2.5}O_{18}H_8$), *Qtz*—quartz ($SiO_2$), *Ms*—muscovite or sericite ($KAl_3Si_3O_{12}H_2$), *Ab*—albite ($NaAlSi_3O_8$), *Mc*—microcline ($KAlSi_3O_8$).

Table 36. Composition of solutions (mol/1000 g H_2O) and equilibrium mineral associations (wt %) in interaction waves 1, 10, 20, and 30

Solution	Wave (NF)				Solution	Wave (NF)			
	1	10	20	30		1	10	20	30
K	1.99e–1	2.01e–1	2.01e–1	2.01e–1	Quartz	32.839	34.353	36.104	37.912
Na	8.78e–1	8.81e–1	8.85e–1	8.85e–1	Pyrrhotite	0.112	–	–	–
Ca	9.83e–3	6.70e–3	5.00e–3	5.01e–3	Galena	0.005	0.004	–	–
Mg	1.91e–5	2.69e–5	3.21e–5	3.22e–5	Sphalerite	0.005	–	–	–
Al	4.19e–5	3.88e–5	3.88e–5	3.88e–5	Chalcocite	–	–	–	–
Si	2.23e–2	2.09e–2	2.09e–2	2.09e–2	Chalcopyrite	0.006	–	–	–
Fe	4.50e–3	4.34e–3	4.08e–3	4.09e–3	Bornite	–	0.003	–	–
Zn	1.81e–4	6.01e–4	–	–	Actinolite	1.098	1.061	1.139	1.197
Pb	1.68e–5	8.19e–5	1.59e–4	–	Muscovite	5.078	6.751	9.004	11.201
Cu	1.27e–5	1.68e–4	2.46e–4	–	Epidot	–	–	0.265	0.897
Cl	1.1	1.1	1.1	1.1	Epidot-60	3.430	1.387	–	–
C	0.5	0.5	0.5	0.5	Epidot-75	–	1.963	2.943	2.191
S(II)	2.16e–2	8.17e–4	2.82e–4	–	Chlorite-75	5.748	5.893	5.761	5.679
pH	0.324	5.304	5.303	5.303	Albite	25.861	28.881	32.239	35.593
Ionic strength	0.633	0.669	0.669	0.669	Microcline	25.819	19.704	12.546	5.331

The pH of the leaching solution (pH 5.3), its ionic strength (0.7), and major-element composition (0.2 *m* K, 0.88 *m* Na, 0.005–0.007 *m* Ca, 0.02 *m* Si, 0.004 *m* Fe, 1.1 *m* Cl, and 0.5 *m* C) remain practically unchanging throughout all waves (Table 36).

The main cause of the changes in the metal concentrations in the leaching solution is the gradual removal of sulfide sulfur from the rock. Until its content remains high enough to maintain concentrations in equilibrium with sulfides, the concentrations of ore elements in the solution do not change. Sulfur removal leads to changes in the equilibrium association of ore minerals in the altered granite (Figs. 51d, 51e). The first sulfide to disappear during leaching is pyrrhotite: it is decomposed after the passage of the first six solution portions through the reactor. While this mineral is present in the system, the solubility of ore sulfides does not increase. This is reflected in plateaus in the concentration trajectories of Zn, Pb, and Cu (Fig. 51a). The minimum in the Pb leaching trajectory at NF = 7 is accounted for by a change from hydrosulfide to chloride Pb complexes, while Zn and Cu chloride complexes dominate throughout the whole range of sulfur concentrations. A strong decrease in the Cu concentration (at waves 2–6) coincides with changes in the equilibrium phase assemblage: the appearance of Fe-poorer epidote (Fig. 51d). A decrease in the sulfide sulfur concentration in the system is clearly reflected in systematic alternations of stable copper sulfides (Figs. 51d, 51e)—chalcopyrite at waves 1–7, bornite at waves 8–12, and chalcocite at waves 11–19—as well as in a rapid increase in the copper concentration in the equilibrium solution (by the onset of wave 7, as much as 93% of sulfur and only 1% of copper are removed from the rock).

The major-component composition of the rock after its reaction with 30 portions of the primary solution is changed as follows (Table 36, Fig. 51f). The quartz content increases (from 33 to 38 wt %), as also do the concentrations of albite (from 26 to 36%) and muscovite or sericite (from 5 to 11%). Simultaneously, the potassic feldspar contents decrease (from 26 to 5%), while the contents of Fe–Mg chlorite and actinolite hardly change (5.6–5.9% and 1.1–1.2%, respectively). The main changes are quite obvious. Inasmuch as the primary solution of this model contains 1 *m* NaCl and 0.1 *m* HCl, its interaction with potassic feldspar leads to the origin of albite, muscovite, and quartz ($4Mc + Na^+ + 2H^+ = Ms + Ab + 6Qtz + 3K^+$). Figure 52 presents the calculation results for model IS-23, whose parameters are analogous to those of the basic model except for the composition of the primary solution (0.5 *m* H_2CO_3, 0.8 *m* NaCl, and 0.2 *m* KCl). The pH of the leaching solutions remains the same as in model IS-2, but the solutions have a lower ionic strength (0.6 as compared with 0.7 in model IS-2) owing to the removal of 0.1 *m* HCl from the primary solution. The introduction of 0.2 *m* KCl results in a practically unchanging composition of the rock after the passage of 30 solution portions (31.9–32.6% quartz, 25.2–25.2% albite, 26.6–28.1% microcline, and 4.63–4.96% muscovite). Comparing Figs. 51a and 52a, and 51f and 52b, one can see that such a significant change in the rock composition in the process of its reaction with solution does not majorly affect the leaching of ore elements.

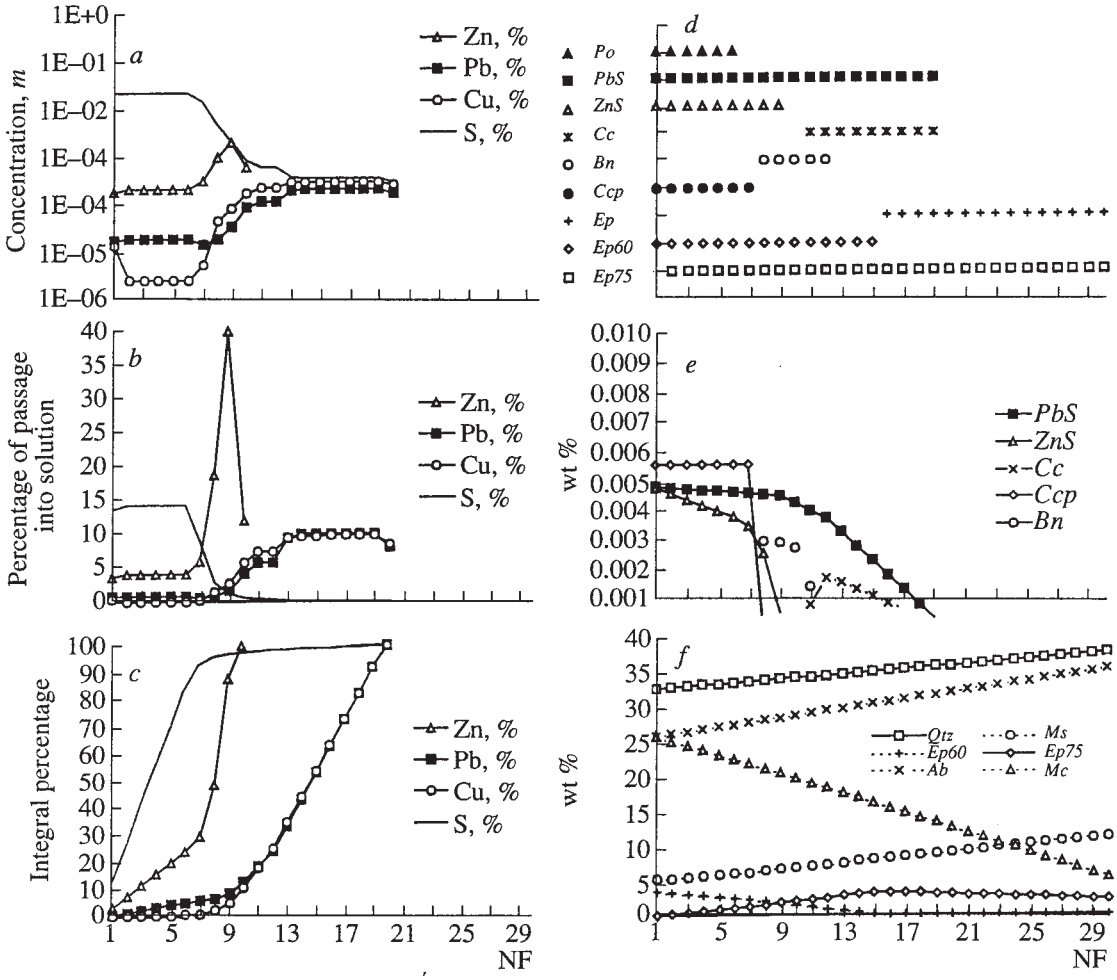

Fig. 51. Basic mobilization model IS-2 (370°C, 1 kbar, 10 kg of granite from the Kholst deposit, the primary solution contains 0.5 *m* H_2CO_3, 1.0 *m* NaCl, and 0.1 *m* HCl). (*a*) Variations in the concentrations (logarithm of molality) of ore elements and sulfide sulfur in the leaching solution as functions of the number of solution portions (waves); (*b*) percentage of component passed into solution from granite at each leaching step; (*c*) integral (sum over waves) percentage of component mobilization; (*d*) ore and minor (<4%) minerals contained in the altered rock and equilibrated with the solution (only minerals present at a current NF are listed); (*e*) equilibrium contents of ore minerals in the altered rock; (*f*) main minerals of the altered rock.

2. Dependence of the mobilization character of ore components on the rock mass in the reactor. All conditions correspond to the basic model (IS-2) except for the original mass of the Kholst granite in the reactor. Figure 53 portrays some calculation results obtained for 5, 10, 20, and 50 kg of rock.

The characteristics of the leaching solutions proportionally vary. It is convenient to compare the results using Figs. 53b and 53b', because they present fragments of data on the basic model with a granite mass of 10 kg (see Figs. 51a, 51c). When the granite mass twice decreases (i.e., to 5 kg), the plateau interval of equal concentrations at low NF is also shortened twice and, correspondingly, the pyrrhotite stability field decreases analogously. An increase in the granite mass by factors of 2 and 5 (to 20 and 50 kg) leads to a roughly two- and fivefold lengthening of this plateau (before NF = 13 and NF = 32, respectively). At the proportionally shifted points, the concentrations of the solutions are fully identical.

Analogous shifts can be seen in the right-hand part of Fig. 53. For instance, similar percentages of total Zn extraction from the rock are achieved at 23.83% in NF = 3 (a'), 23.67% in NF = 6 (b'), 23.62% in NF = 12 (c'), and 23.70% in NF = 30 (d').

When 30 portions of the primary solution are passed through the reactor with 50 kg of granite, the association of minerals with pyrrhotite remains stable, and the composition of the system favorable for a strong increase in the concentrations of metals in the solution is not achieved. Of course, further interaction leads to the effects identified at smaller rock masses (the metals are fully leached at wave 96).

3. Dependence of the mobilization character of ore components on the rock composition in the reactor. The parameters of the basic model are preserved, but the

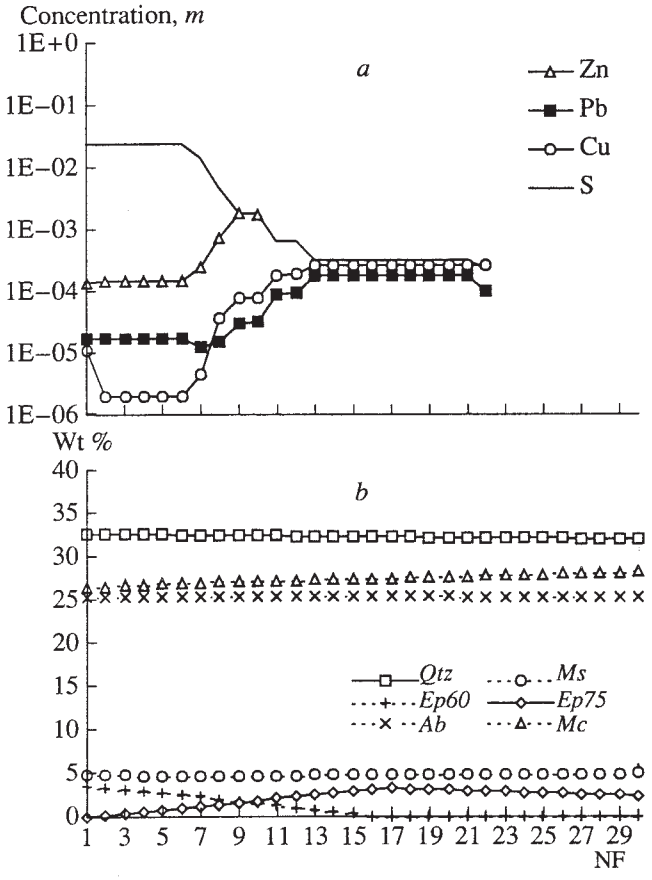

Fig. 52. Mobilization model IS-23 (370°C, 1 kbar, 10 kg of granite from the Kholst deposit, the primary solution contains 0.5 *m* H_2CO_3, 0.8 *m* NaCl, and 0.2 *m* KCl). (*a*) Variations in the concentrations (logarithm of molality) of ore elements and sulfide sulfur in the leaching solution as functions of the number of solution portions (waves); (*b*) main minerals of the altered rock.

calculations and comparisons of the results are conducted for granites from the Kholst and Verkhnii Zgid deposits (see Table 35 for the compositions). Figure 54 illustrates the calculation results obtained for the V. Zgid granite, which are compared with analogous data for granite from the Kholst deposit (Fig. 51).

The comparison of Figs. 51a, 51c, and 51d with Figs. 54a, 54a', and 54a" demonstrates that the mobilization character of ore components from these rocks differs even if the leaching conditions remain the same. When the primary solution interacts with the V. Zgid granite (Fig. 54a), the Zn, Pb, and Cu concentrations do not increase rapidly. The extraction of Zn outstrips S leaching (as much as 100% of Zn and as little as 45% of S in NF = 16), the sulfide sulfur concentration decreases only fourfold after the passage of 30 solution portions, and the overall extraction of Pb and Cu amounts to 23 and 5%, respectively, of their original contents in the rock. It is reasonable to suggest that the differences are predetermined by the differences between the compositions of the Kholst and V. Zgid granites. The data of Table 37 indicate that the compositions of the altered rocks are practically identical. Nevertheless, there are small but important differences in minor minerals, whose appearance is indicative of differences between the leaching conditions. The most important of these differences is the occurrence of pyrite in the equilibrium mineral assemblage produced by the reaction of the primary solution with the V. Zgid granite (Fig. 54a", Table 37).

The occurrence of pyrite indicates that the V. Zgid granite contains more sulfide sulfur than the Kholst granite. Indeed, the $Fe_S/(Fe_S + FeO)$ ratio in the V. Zgid granite is 12.44 mol %, and this ratio for the Kholst granite is 2.51 mol %. According to Gotman and Malakhova [1966] (Table 35), analyses of the V. Zgid granites were averaged using the results of sampling near and away from vein bodies, and all samples near veins contained more than 0.15 wt % (up to 0.5%) sulfide sulfur. The sulfide sulfur contents analyzed away from veins approached those in the Kholst granite, i.e., ~0.05–0.07 wt %.

We checked whether the V. Zgid granite contains "excess" sulfur by conducting additional calculations, in which the $Fe_S/(Fe_S + FeO)$ ratio in the granite was modified (the amount of sulfide sulfur was decreased and the amount of oxide iron was increased at the same total iron content). These data are portrayed in Figs. 54b, 54c in which $Fe_S/(Fe_S + FeO)$ ratio is 4.61 and 2.3%. Comparison between Figs. 54c (c' and c") and 51a (c, d) indicates that an increase in the sulfide sulfur concentration affects the character of mobilization of ore components from the V. Zgid granite and brings it to a form virtually analogous to the leaching character from the Kholst granite. Of course, minor differences still persist. For example, because of the lower Fe content in the V. Zgid granite, pyrrhotite remains stable in it only in NF from 1 to 3. Still, the general tendency of the mobilization of components retains a characteristic form, the same as in the basic model.

4. Effect of temperature on the character of mobilization of ore components. All parameters except temperature are analogous to those in model IS-2. The calculations are conducted for temperatures of 250 and 420°C. The results obtained for ore components are partly shown in Fig. 55. The most important consequence of the temperature decrease in the reactor is a decrease in the solubility of sulfides ore elements contained in the granite, as a result of which the character of the leaching process is also modified. For example, for the first solution portion (NF = 1), the Zn concentrations at temperatures of 420 and 250°C are, respectively, 2.15×10^{-3} and 1.26×10^{-6} *m*, i.e., a difference by a factor of 1700. The analogous values for Pb are 4.82×10^{-5} and 7.68×10^{-7} *m* (a difference by a factor of 60); these values for Cu are 3.03×10^{-5} and 9.45×10^{-8} *m* (a difference by a factor of 320); and for sulfide S, 4.35×10^{-2} and 2.65×10^{-3} *m* (a difference by a factor of 15).

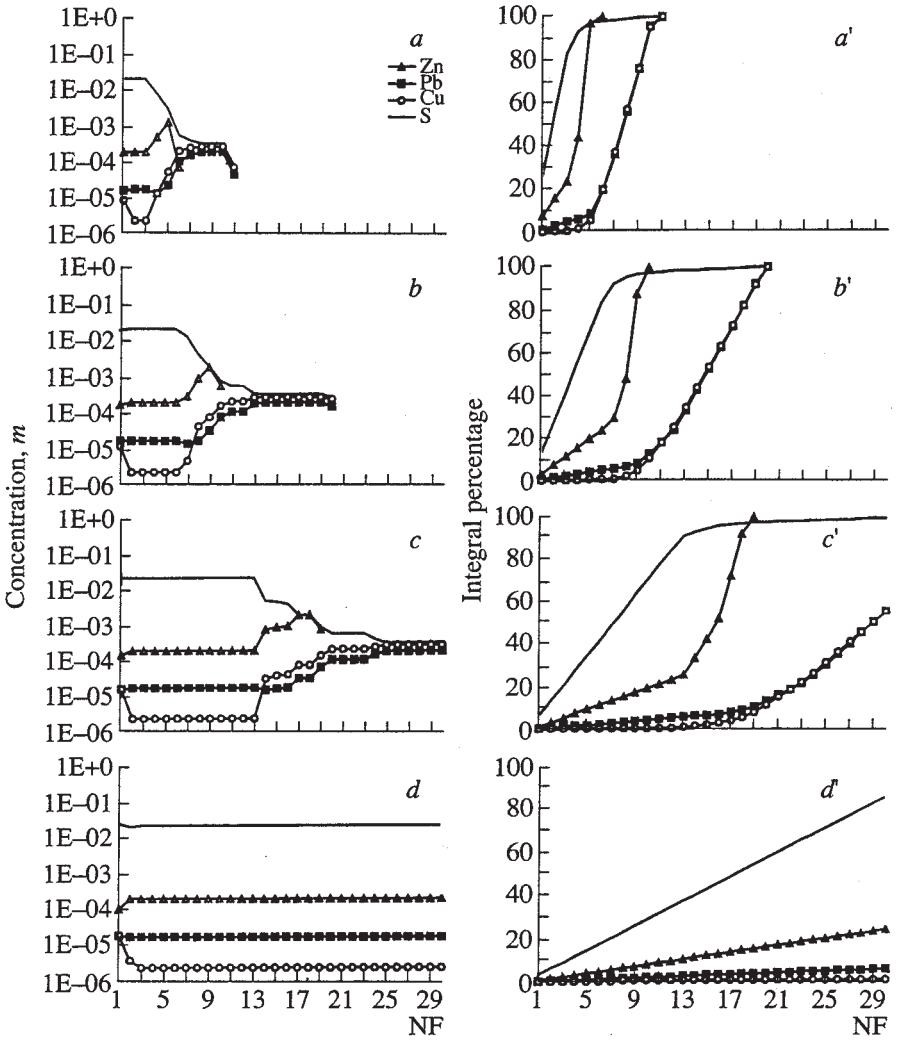

Fig. 53. Dependence of the mobilization character of ore components on the rock mass in the reactor (model IS-2, granite from the Kholst deposit). (*a*, *a'*) 5 kg, (*b*, *b'*) 10 kg, (*c*, *c'*) 20 kg, (*d*, *d'*) 50 kg.

The leaching character at different temperatures can be compared using the plots in Fig. 55 (the trajectories for 370°C correspond to the basic model). A temperature increase to 400 or 420°C results in a decrease in the number of primary solution portions at which ore sulfides are retained in the rock. For example, at 400°C sphalerite remains stable until NF = 4, while galena and Cu sulfides are stable up to NF = 11. At 420°C sphalerite is stable to NF = 2, and galena and Cu sulfides persist to NF = 8. A temperature decrease shifts the stability boundary of sulfides toward greater NF. For example, these values for Zn are 9 at 370°C, 11 at 360°C, 14 at 350°C, 18 at 340°C, 23 at 330°C, 41 at 320°C, 57 at 310°C, 70 at 300°C, 86 at 280°C, and more than 100 at 250°C. The shifts for Pb and Cu are analogous, but their NF are 10–20 units greater. Correspondingly, the plateaus of the maximum concentrations of the metals are also shifted relative to NF: no plateaus occur at NF from 1 to 30 at temperatures below 330°C.

There are certain differences between the equilibrium mineral assemblages. At temperatures of 360–420°C, the association is the same as in the basic model (the only difference is NF). At temperatures of 340–350°C, pyrite appears (at NF from 2 to 8–10). At temperatures of 250–300°C, calcite is added to the equilibrium mineral assemblage (in amount of 0.1–1.6 wt %).

5. Effect of pressure on the character of mobilization of ore components. The calculations were carried out at temperatures of 370, 400, and 420°C and pressures of 400, 600, 800, and 1000 bar for the same primary solution and rock as in the basic model. Figure 56 makes it possible to compare the calculation results (the plots represent the degree of metal extraction at a given NF as percent of its original mole concentration in the rock).

A pressure decrease at any temperature brings about the following effects:

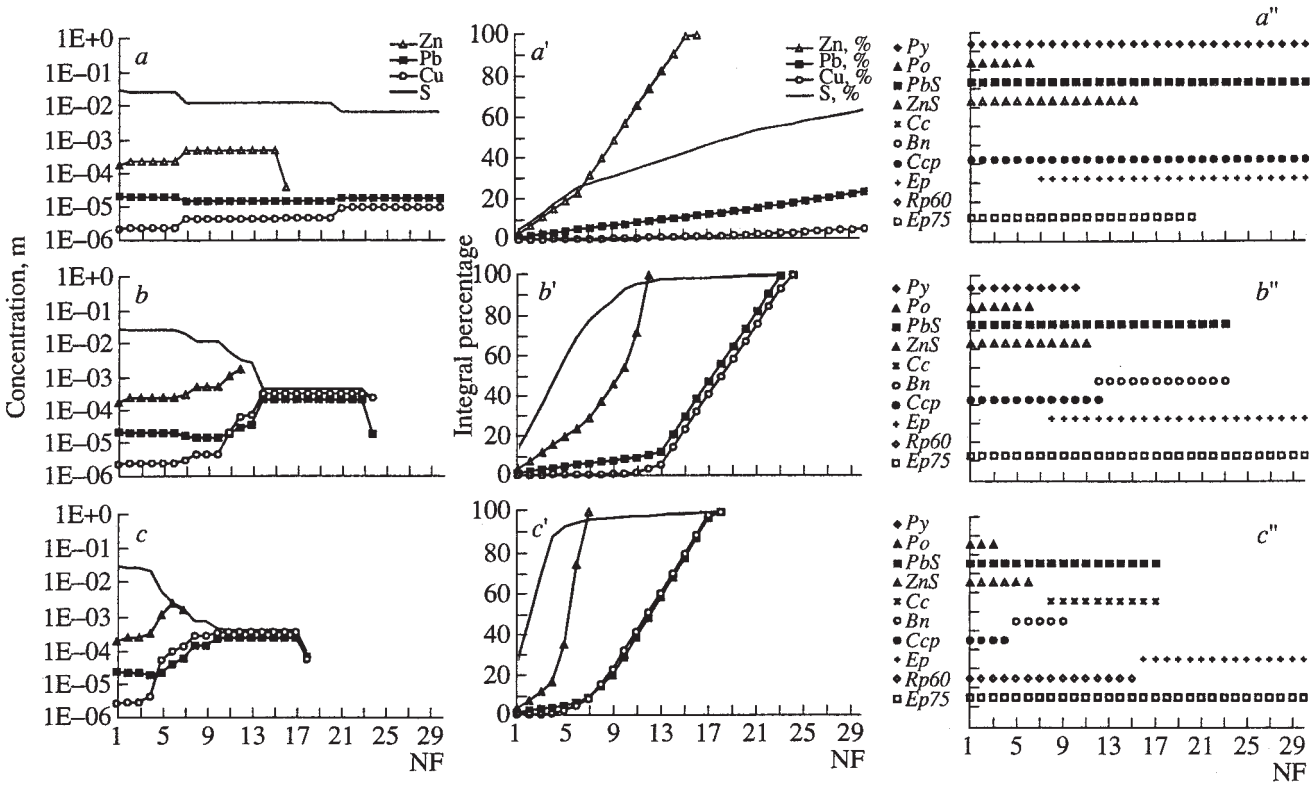

Fig. 54. Dependence of the mobilization character of ore components on the concentration of sulfide sulfur in granite from the Verkhnii Zgid deposit (10 kg, 370°C, 1 kbar). (*a*, *a*', *a*") 0.054 gram atom/kg rock (or 0.17%, Table 6.1); (*b*, *b*', *b*") 0.02 gram atom; (*c*, *c*', *c*") 0.01 gram atom.

* the concentration of the metal in the solution increases;

* the NF at which the metal is completely extracted from the rock decreases;

* the maxima of passage of the ore elements into solution are differentiated between waves.

The increase in the concentrations with the pressure decreasing from 1000 to 600 bar is smaller than the analogous effect during a temperature increase from 370 to 420°C. For example, an analogous temperature increase at P = 1000 bar results in the following increase in the concentrations (for wave 1): from 1.81×10^{-4} to 2.15×10^{-3} m for Zn, or from 3.6 to 43% passage of this metal into solution (an increase by a factor of 12); from 1.68×10^{-5} to 4.82×10^{-5} m for Pb, or from 0.8 to 2.4% passage into solution (an increase by a factor of ~3); and from 1.27×10^{-5} to 3.03×10^{-5} m for Cu, or from 0.4 to 1.0% passage (an increase by a factor of 2.4). Considering data on leaching at a constant temperature (370°C) and decreasing pressure (from 1000 to 600 bar), the increase in the passage into solution (for wave 1) is from 3.6 to 18.6% (by a factor of ~5) for Zn, from 0.8 to 1.3% (by a factor of ~1.6) for Pb, and practically unchanging figures for Cu. Analogous values at 420°C are from 42.9 to 100% for Zn, from 2.4 to 6.6% for Pb, and a slight decline for Cu in the first waves and then a subsequent increase.

Figure 56 demonstrates that a pressure decrease is favorable for differentiation between the leaching maxima of the metals, with the succession of mobility assuming the form Zn > Pb > Cu. For example, at 1000 bar, the maxima of Pb and Cu leaching virtually coincide, so that both metals are extracted from the rock simultaneously (in the same NF). At 600 bar, the maxima of Pb and Cu fall onto NF equal to 13 and 15, respectively, at 370°C; NF equal to 7 and 9 at 400°C; and NF equal to 5 and 7 at 420°C. The shifts in the maxima are coupled with an increase in the percentage of metal extraction into solution. For example, at 600 bar and 370°C, when Pb is already completely removed from the rock, this rock still contains up to 25% of its original Cu content (up to 40% of Cu at 400 bar), and the analogous values for 400 and 420°C are, respectively, up to 42 and up to 45% of the Cu contents.

The equilibrium mineral assemblages change with decreasing pressure according to the increase in the solubility but remain generally similar to the assemblages in the basic model. The exceptions is the appearance of pyrite at 370°C and pressures of 400–600 bar (NF from 2 to 5) and magnetite at 420°C and a pressure of 600 bar (NF = 23 and greater).

Table 37. Equilibrium mineral associations (wt %) that were produced in granites from the Kholst and V. Zgid deposits during their interaction with 1 and 30 portions of the primary solution*

Mineral	Wave 1		Wave 30	
	granite from Kholst	granite from V. Zgid	granite from Kholst	granite from V. Zgid
Qtz	32.839	33.702	37.912	38.958
Ab	25.861	24.856	35.593	34.410
Mc	25.819	28.991	5.331	8.461
Act	1.098	0.985	1.197	1.019
Ms	5.078	3.912	11.201	10.011
Chl75	5.748	3.402	5.679	3.438
Ep60	3.430	0	0	0
Ep75	0	3.790	2.191	0
Ep	0	0	0.897	3.574
Py	0	0.219	0	0.120
Po	0.112	0.129	0	0
PbS	0.005	0.005	0	0.004
ZnS	0.005	0.005	0	0
Ccp	0.006	0.006	0	0.005

*The primary solution and leaching conditions are the same as in the basic model IS-2.

6. Effect of the primary solution composition on the character of mobilization of ore components. The calculations were conducted at 370°C and 1 kbar for 17 different compositions of the primary solution (Table 38). The variations in the concentrations of solution components were as follows: from 0 to 0.5 *m* for H_2CO_3, from 0 to 0.7 *m* for $NaHCO_3$, from 0.4 to 1.0 *m* for NaCl, and from 0 to 0.3 *m* for $CaCl_2$. In a few instances we specified HCl = 0.1 *m* (basic model IS-2) and H_2S = 0.001 *m* (model IS-3). In all models but the basic one, the bulk Cl concentration in the system was 1 *m*.

The results are significantly different, because the compositions of the systems also notably vary. It is convenient to analyze them by groups, within which the composition of the primary solution varies systematically.

Group 1. In this series the concentrations of a number of components vary simultaneously: as the $CaCl_2$ concentration increases from 0.05 to 0.3 *m*, H_2CO_3 decreases and $NaHCO_3$ increases (at a constant ΣC = 0.5 *m*) and NaCl decreases from 0.8 to 0.4 *m* (at ΣCl remaining constant and equal to 1.0 *m*).

The general leaching succession resembles that in the basic model (compare Fig. 51a with Figs. 57a and 57b). However, the introduction of components that were absent from the basic model ($CaCl_2$ and $NaHCO_3$) brings about changes in the equilibrium mineral assemblages and an increase in the pH (at NF = 29–30, pH is 5.8 in model IS-11 and 6.0 in model IS-13). The solubility of Cu and Pb sulfides somewhat decreases (as can be clearly seen at NF > 15). The decrease in the solubility is unequal for Pb and Cu. In the basic model, Pb and Cu sulfides are completely dissolved simultaneously in NF = 19. In model IS-11, Cu minerals disappear in NF = 22 and galena disappears in NF = 23. Further changes in the composition of the solutions in this group result in an even more pronounced differentiation between these metals: in model IS-13 (Fig. 57b), the values of NF for Cu and Pb are, respectively 24 and 28.

Changes in the primary solution composition lead to the appearance of minerals that did not form in the basic model. For example, during the final leaching stage in model IS-13 (as well as in IS-6, Table 38), calcite starts to crystallize (in NF = 25–29). An increase in the Ca concentration in the solution and its strong alkalinity result in an increase in the contents of Ca silicates (actinolite and epidote), which, in turn, modifies the chlorite: Fe-chlorite appears, while the stability region (in terms of NF) of Fe–Mg chlorite decreases. In contrast to the basic model, muscovite is stable only to NF = 14–16 and the albite and microcline contents are much higher (for example, in model IS-13 after the passage of 30 waves of the primary solution, the albite and microcline contents are, respectively, 40 and 15 wt %).

Group 2. In this series, the concentrations are constant for $CaCl_2$ (0.1 *m*) and NaCl (0.8 *m*). At a constant H_2CO_3 concentration (excluding model IS-12), the $NaHCO_3$ concentration increases: the $H_2CO_3/NaHCO_3$ ratio changes from 1.5 in model IS-10 to 0.5 in model IS-20 (ΣNa increases from 1.0 to 1.4 *m*, while ΣCa increases from 0.5 to 0.9 *m*; Table 38).

While the first model of this group (model IS-10, Fig. 57c) yields results close to those of the basic model, the final models significantly differ (for exam-

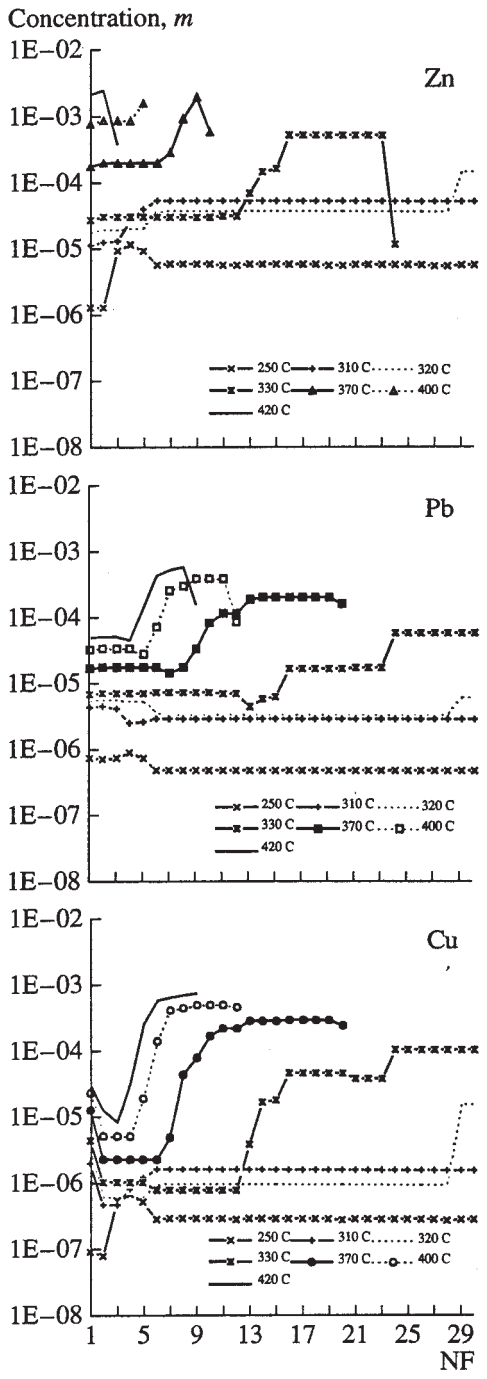

Fig. 55. Temperature dependence of the mobilization character of ore components. Other conditions are as in model IS-2.

ple, IS-19, Fig. 57d). This group of models is characterized by the following features:

* the pH significantly increases (to 7.7–7.8) in NF = 30 (for example, in model IS-19),

* sulfate sulfur appears in the equilibrium solutions in amounts greater than those of sulfide sulfur (at $H_2CO_3/NaHCO_3$ = 3/5 in model IS-19 in NF = 25 and further, at $H_2CO_3/NaHCO_3$ = 3/6 in NF = 21):

* the solubility of ore sulfides significantly diminishes.

The following features are characteristic of the equilibrium association of solid phases:

* magnetite is formed (starting from NF = 25 in model IS-17, from NF = 12 in model IS-19, and from NF = 9 in IS-20);

* calcite appears at lower degrees of interaction than in group 1 (in NF = 10 and greater in IS-19);

* the albite content is very high: 48.3, 54.9, 57.7, and 58.3 wt % in NF = 30 in models from IS-17 to IS-20, respectively;

* chlorite and epidote stability systematically decreases (for example, they are present in model IS-19 only in NF = 23).

This reaction of the system to variations in the composition of the primary solution leads to a significant decrease in the percentage of integral leaching of ore elements during the 30 interaction events. For example, in model IS-19, Zn is extracted completely at NF = 22, while the extraction percentages of Pb, Cu, and S by NF = 30 are, respectively, 16.7, 41.4. and 98.4%. The decrease in the degree of leaching is even stronger in model IS-20: in NF = 30, the leaching of Zn, Pb, Cu, and S attains, respectively, 43.6, 7.3, 16.8, and 96.7%. Hence, an increase in the $NaHCO_3$ concentration in the primary solution changes the leaching succession from Zn ≫ Pb = Cu to Zn > Cu > Pb.

Group 3. At constant concentrations $CaCl_2$ and NaCl (0.2 and 0.6 *m*, respectively), the concentration of $NaHCO_3$ increases from 0.3 to 0.7 *m* in the absence of H_2CO_3 (ΣNa increases from 0.9 to 1.3 *m*, and ΣC increases from 0.3 to 0.7 *m*; Table 38). The results of calculations for two solutions are summarized in Figs. 57e and 57f.

The general leaching tendency is close to that described above for the group-2 solutions, although there are also some significant differences. The most important of them are as follows:

* sulfate sulfur predominates over sulfide sulfur during the earliest interaction stages (starting from NF = 19 in model IS-9);

* the solubility of sulfides drastically increases during the closing leaching stages, with the transition of the system to an oxidized state, which is characterized by the appearance of hematite in the equilibrium mineral association (hematite is formed in models IS-7, IS-8, and IS-9);

* calcite and magnetite appear earlier than in other models with the same ΣC (for example, calcite becomes stable in NF = 14 in model IS-18 and NF = 8 in model IS-9), with the calcite content in NF = 30 sometimes reaching as high as 6 wt %.

These features result in unusual configurations of the mobilization trajectories (Fig. 57f). Obviously, if

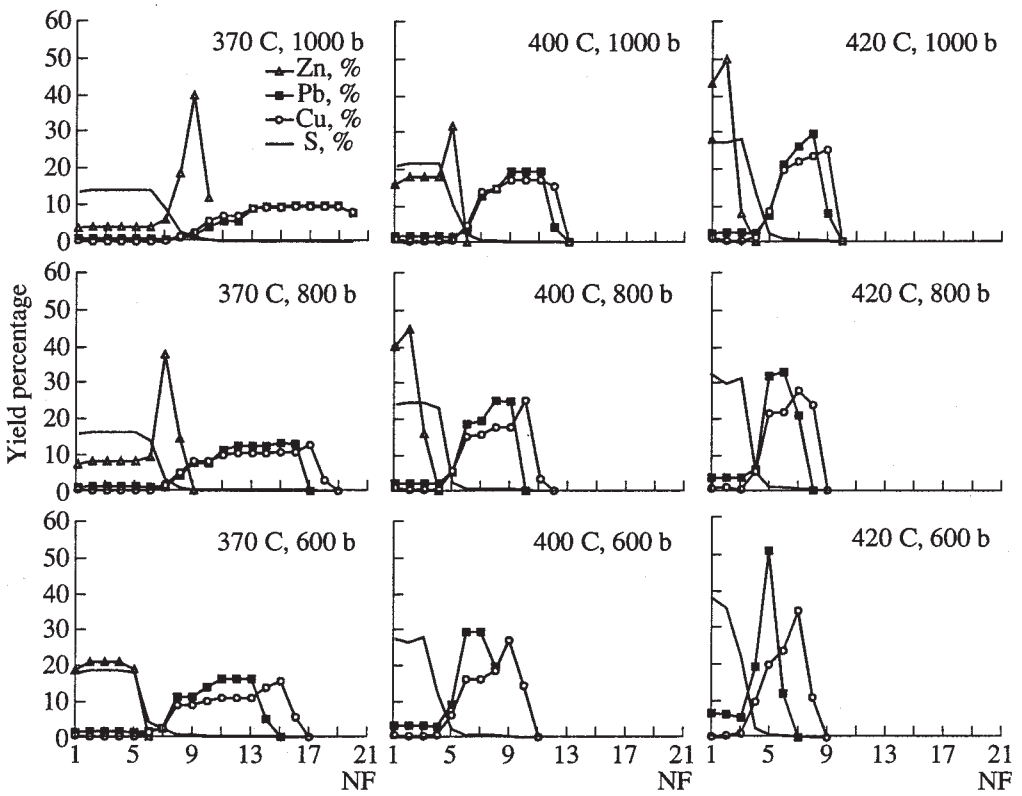

Fig. 56. Pressure dependence of the mobilization character of ore components (absence of Zn at 400°C, 600 bar and 420°C, 600 and 800 bar—100% removal of the metal at NF = 1).

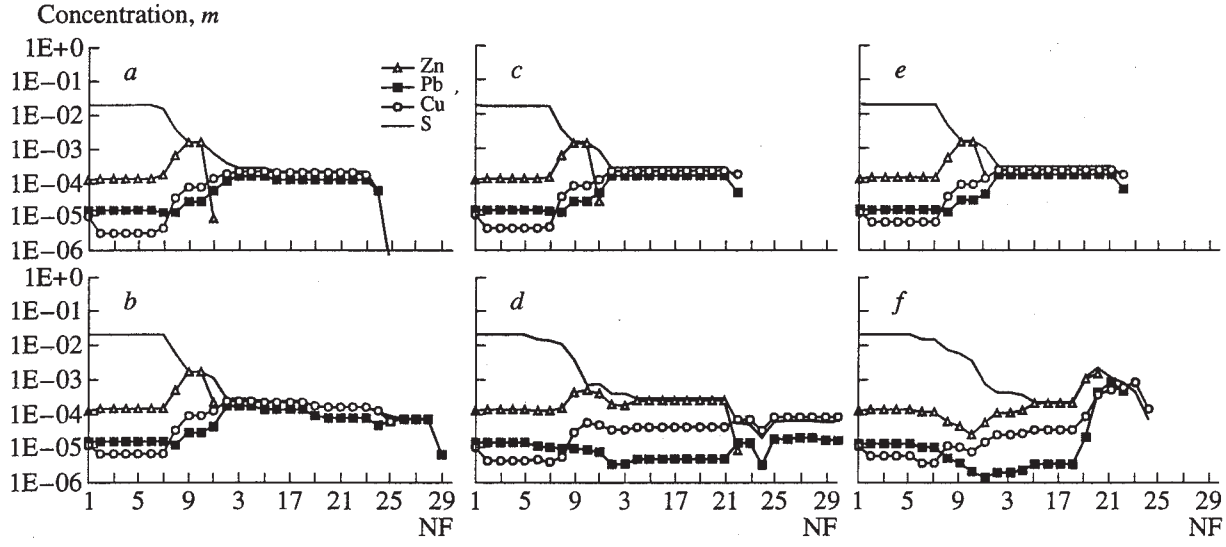

Fig. 57. Effect of the primary solution composition on the character of mobilization of ore components (370°C, 1 kbar). (*a, b*) Group 1, models IS-11 and IS-13; (*c, d*) group 2, models IS-10 and IS-19; (*e, f*) group 3, models IS-16 and IS-9.

there were no jumps in the solubility of sulfides during hematite formation, the leaching succession of the metals remained Zn > Cu > Pb. However, this drastic increase modifies mobilization succession to a form close to that in the basic model: Zn > Pb > Cu (for example, the NF of Zn, Pb, and Cu in model IS-9 is equal to, respectively, 19, 21, and 23).

It should be emphasized that external conditions (temperature and pressure) can modify the leaching pattern in a major way. Figure 58 offers an example of this effect. Model IS-12 (group 2, see Table 38 and Figs. 58a, 58b) shows a complicated mobilization pattern at P = 1000 bar, but a pressure decrease to 600 bar transforms it into a close analogy of the basic model

Table 38. Primary solution compositions (mol/1000 g H_2O)

Model	H_2CO_3	$NaHCO_3$	NaCl	$CaCl_2$	ΣNa	ΣC	ΣCa
			Group 1				
IS-11	0.3	0.2	0.8	0.05	1.0	0.5	0.05
IS-10	0.3	0.2	0.8	0.1	1.0	0.5	0.1
IS-14	0.2	0.3	0.7	0.15	1.0	0.5	0.15
IS-13	0.1	0.4	0.6	0.2	1.0	0.5	0.2
IS-6	–	0.5	0.4	0.3	0.9	0.5	0.3
			Group 2				
IS-10	0.3	0.2	0.8	0.1	1.0	0.5	0.1
IS-12	0.2	0.3	0.8	0.1	1.1	0.5	0.1
IS-17	0.3	0.3	0.8	0.1	1.1	0.6	0.1
IS-18	0.3	0.4	0.8	0.1	1.2	0.7	0.1
IS-19	0.3	0.5	0.8	0.1	1.3	0.8	0.1
IS-20	0.3	0.6	0.8	0.1	1.4	0.9	0.1
			Group 3				
IS-16	–	0.3	0.6	0.2	0.9	0.3	0.2
IS-15	–	0.4	0.6	0.2	1.0	0.4	0.2
IS-7	–	0.5	0.6	0.2	1.1	0.5	0.2
IS-8	–	0.6	0.6	0.2	1.2	0.6	0.2
IS-9	–	0.7	0.6	0.2	1.3	0.7	0.2

(the mobilization order thereby changes from Zn > Cu > Pb to Zn > Pb > Cu). Model IS-3 (Figs. 58c and 58d; solution composition: H_2CO_3 = 0.5 *m*, NaCl = 1 *m*, H_2S = 0.001 *m*) shows Pb and Cu mobilization significantly spread over NF at 370°C and spanning a much narrower NF range at 400°C.

Groups 1–3 comprise primary solutions with ΣCl = 1 *m*, but the total concentration was sometimes much higher than one. For comparison, let us consider data on a reaction with a solution whose concentrations are twice lower than in the primary solution of the basic model (model IS-24. Fig. 59). A twofold decrease in the bulk Cl concentration (to 0.55 *m*) leads to a drastic decrease in the solubility of sulfides as compared with model IS-2. The corresponding figures for NF = 1 are as follows: 2.36×10^{-5} and 1.81×10^{-4} *m* for Zn (a decrease by a factor of 7.7), 1.48×10^{-5} and 1.68×10^{-5} *m* for Pb (a decrease by a factor of 1.1), and 5.79×10^{-6} and 1.27×10^{-5} *m* for Cu (a decrease by a factor of 2.2). The changes in the solubility of sulfides result in the expansion of complete leaching intervals: to NF = 17 for Zn, NF = 41 for Pb, and NF = 44 for Cu, i.e., instead of Zn ≫ Pb = Cu of the basic model, model IS-24 has a succession Zn ≫ Pb > Cu.

6.1.3. Discussion of the results

1. Our simulations indicate that interaction between the primary barren solutions and granite at 310–420°C and 0.4–1.0 kbar results in high-temperature metalliferous solutions, which can potentially serve as initial solutions for the hydrothermal system in question. Our results are in good agreement with experimental data [Hemley *et al.*, 1992], although the experiments were conducted in another system: synthetic quartz–muscovite–potassic feldspar buffer in the presence of a pyrite–pyrrhotite–magnetite–sphalerite–galena–chalcopyrite assemblage in a system without solution exchange. For example, our basic model (370°C, 1 kbar) yields 1.8×10^{-4} *m* Zn early in the course of leaching and 2×10^{-3} *m* Zn during the final stages, but the solution still could potentially dissolve this metal. In experiments at 1 kbar, the average concentration was 1.4×10^{-3} *m* at 350°C and $5.1–8.2 \times 10^{-3}$ *m* at 400°C. The calculated value for Pb is a slight underestimation: 2×10^{-4} *m* as compared with the experimental value of 6×10^{-4} *m* at 350°C. The calculated and experimental values for Cu are practically identical: 2.9×10^{-4} and 3.4×10^{-4} *m*. This agreement testifies to the high reliability of our calculations.

2. One of the most important results obtained using our mobilization models is the establishment of a significant increase in the concentrations of ore elements with time in the process of leaching without any changes in the external conditions. The concentrations of the metals can thereby attain values (from $n \times 10^{-3}$ to $n \times 10^{-4}$ *m*) that are more than one order of magnitude higher than the concentrations after a single interaction episode in a water–rock system. This effect was described above (Chapter 2, Section 2.4) with reference to the basic model. The result is interesting in two

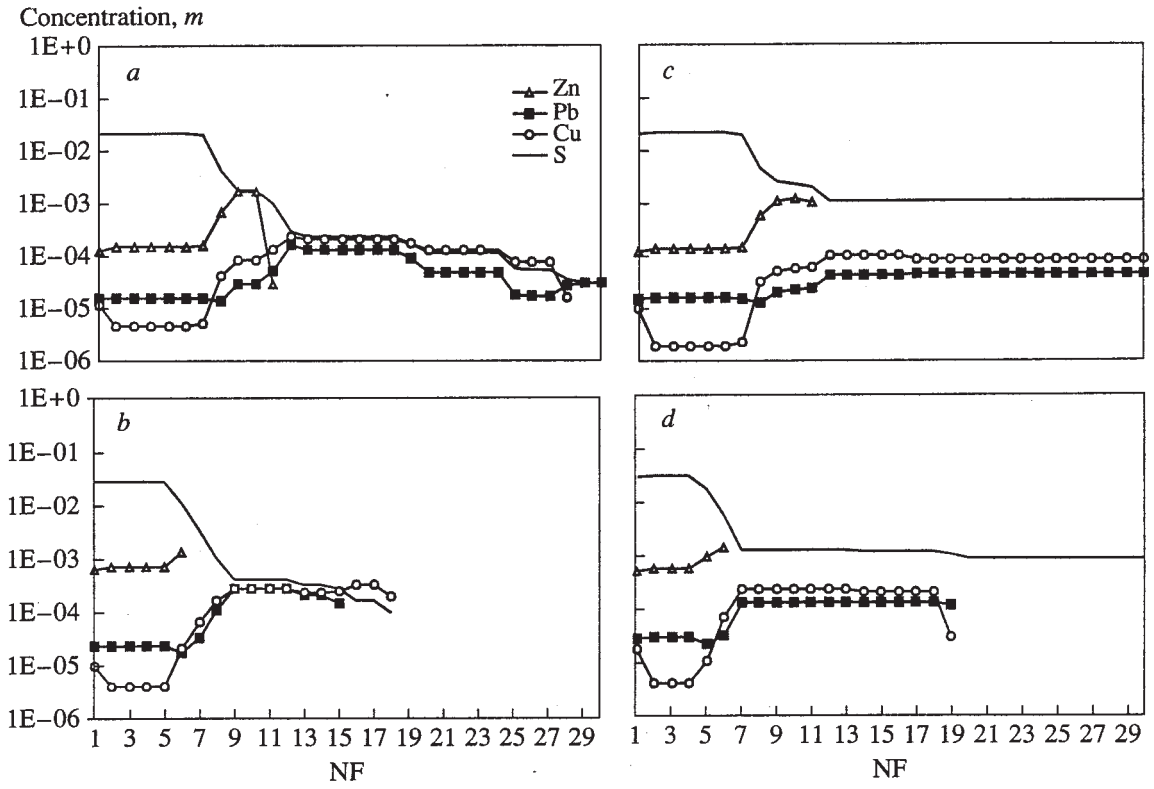

Fig. 58. Variations in the character of mobilization of ore components in systems with different primary solutions at decreasing pressure or increasing temperature. Model IS-12: (*a*) 370°C, 1000 bar; (*b*) 370°C, 600 bar; model IS-3: (*c*) 370°C, 1000 bar; (*d*) 400°C, 1000 bar.

aspects. First, the ore-forming potential of the solution appears to be "enhanced" with time, and, second, ore components can, in principle, be used to trace the compositional evolution of the hydrothermal solution within a given stage, whereas the concentrations of other components remain almost unchanged.

3. The efficiency of the process is unequal in systems with different temperatures and the composition of their primary solutions. At high temperatures, mobilization proceeds quite quickly (over NF < 30). At temperatures of 310–320°C, leaching is more sluggish (for example, the complete extraction of metals at 250°C is attained only at NF > 100) and the concentrations of ore components in the equilibrium solutions are very low (from $n \times 10^{-6}$ to $n \times 10^{-7}$ *m*) at cumulative rock/water ratios from 10 to 0.1. In application to the deposits discussed here, it is reasonable to suggest fairly high temperatures in the mobilization region, because, according to Lyakhov *et al.* [1978, 1994], the highest temperatures inferred from inclusion in the gangue quartz of the mineral stage are only rarely lower than 330–340°C. Hence, it is logical to admit that the temperature in the mobilization zone should have been $n \times 10$°C higher. However, such a temperature extrapolation to the mobilization zone implies that this region has a temperature that changes relatively little. If this region was elongated updip the Sadon–Unal fault and its significant splay structures (as was assumed above), the mobilization zone should have been characterized by a temperature gradient, so that leaching within this region should have proceeded in somewhat different manners depending on the position of the leaching site. More deeply seated sites were characterized by higher temperatures than those sitting at shallower depths, which could result in the development of lateral zoning in the mineralized veins in response to differences in the solubility, etc. There are indirect lines of evidence in support of this idea: lateral temperature gradients in veins as high as 6°C per 100 m along strike were documented by Lyakhov *et al.* [1978], with the maximum gradient (zoning in the vein plane) in the concentrations of ore elements detected in the direction from the lowermost levels of the southwestern flank, adjacent to the Sadon–Unal fault, to the upper levels of the northeastern flank of the Sadon deposit [Grigoryan, 1992]. Lyakhov *et al.* [1994] and Laz'ko *et al.* [1981] also noted that the time span of the mineral stage was characterized by a gradual decrease in the hydrothermal fluid temperature; i.e., it is reasonable to assume that the temperature in the mobilization region also decreased in the process of leaching. Figure 60 presents two variants of models for a gradual temperature decrease in the reactor (the reference model is the basic model here).

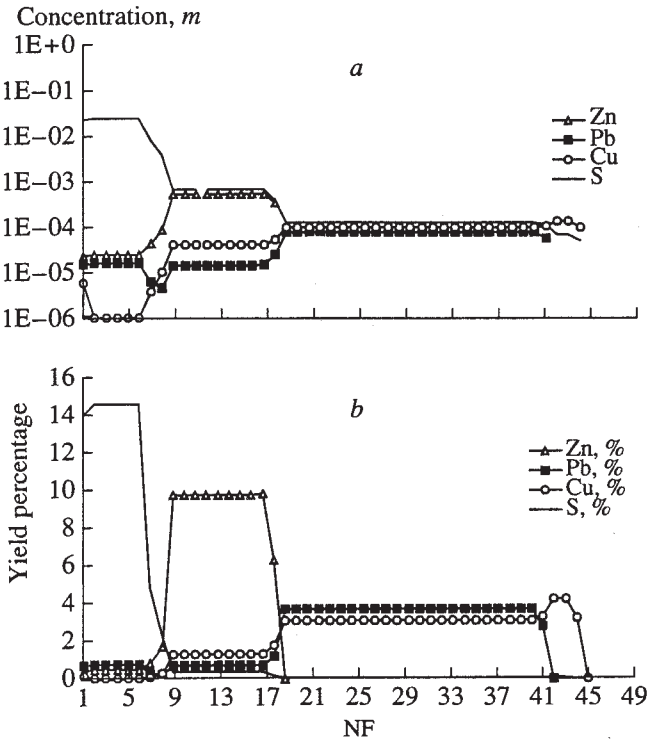

Fig. 59. Variations in the mobilization character of ore components with a twofold decrease in the concentration of the primary solution of the basic model (model IS-24, 370°C, 1000 bar).

It can be seen that, depending on the rate of temperature decline, the mobilization character can vary significantly (Figs. 60a and 60b indicate that, at the integral $\Delta T = 50$°C, every five successive waves or portions of the primary solution have temperatures of 370, 360, 350, 340, 330, and 320°C; in Figs. 60c and 60d, the integral $\Delta T = 120$°C, and every five successive waves or portions of the primary solution have temperatures of 370, 350, 330, 310, 280, and 250°C). It follows that, in addition to the possible temperature gradient updip the mobilization zone, it is quite probable that the temperature gradually decreased at every topographical level where the leaching processes took place.

4. The composition of the primary solution can strongly affect the character of the solubility of sulfides contained in the granite, and, consequently, there cannot be an increase but a decrease in the concentrations of metals in successive solution waves (see point 6 of the results), although this phenomenon is quite rare in the models examined here. Examples of such situations are offered by models IS-19 (group 2) and IS-9 (group 3), which are characterized by ΣNa concentrations greater than 1.2 *m* and high overall mineralization of the solutions. However, even in these models, the decrease in the metal concentrations is clearly pronounced only for Pb and is usually of local character in terms of NF. Analyses of aqueous extracts and cryometry of fluid inclusions (mostly in the gangue quartz) indicate [Lyakhov *et al.*, 1994] that the hydrothermal solution was of chloride–hydrocarbonate sodic–calcic composition and has a bulk concentration of dissolved salts no higher than 20–24% NaCl equivalent, most often below $n \times 1\%$. Our solutions have bulk concentrations from 7.6 to 11.3%. The solution of model IS-24 (twice-diluted solution of the basic model) has a bulk concentration of 4.4%. Thus, the concentrations of the solutions are in good agreement with data on the deposits. However, these are facts that seem to constrain the possible compositional range of the primary solution. First, this is the amount of albite that forms when the primary solution interacts with granite. Some of our models (IS-8, IS-9, IS-18, IS-19, and IS-20) yield >50 wt % albite after the passage of approximately 30 waves of the primary solution. No appreciable increase in the albite content was described either near the possible mobilization zones (level XIV at V. Zgid, according to the data of Chapter 5 [Borisov, 1997]) or in the wall-rock metasomatics. Observations of this type seem to constrain the ΣNa concentration in the primary solution to ≤1.0 *m*. Second, according to [Laz'ko *et al.*, 1981], the pH variations in quartz populations belonging to different stages are, at room temperature, 6.25–7.95. In the models mentioned above, pH at 370°C and 1 kbar corresponds to 6.8–7.8 and, obviously, this solution should become much more alkaline with decreasing temperature.

5. The metalliferous potential of the leaching solutions significantly varies in the course of mobilization processes. This is principally consistent with the results of our geochemical research (see Chapter 5). Most of our models are characterized by the same leaching order of metals: Zn predominates in the solution early in the course of this process and is followed by Pb and Cu, i.e., Zn ⩾ Pb ≥ Cu.[16] The solution during the final stages is barren. This result obviously implies that the ore-forming process terminates as soon as the ore material is completely depleted in the source. Therewith the temperature, pressure, and the composition of the solution can remain unchanged. The hydrothermal process can go on but only as a barren one: growth of the quartz core of the vein, carbonatization, redeposition of earlier ore minerals, recrystallization and, perhaps, partial removal of the material. The ore-forming process can be resumed only if the zone where the ore elements are mobilized is modified, usually during a new pulse of tectonic activity, as is typical of both our or any other deposits.

6. The established leaching succession is particularly interesting, because Cu mineralization at the deposits is quantitatively subordinate. Chalcopyrite is

[16]Here and below, the signs >, ≥, and = denote the leaching order of ore elements when the barren solution reacts with granite (starting from the onset of leaching until the metal is completely removed from the rock). The sign ⩾ means that this element significantly surpasses the leaching of other elements in terms of NF.

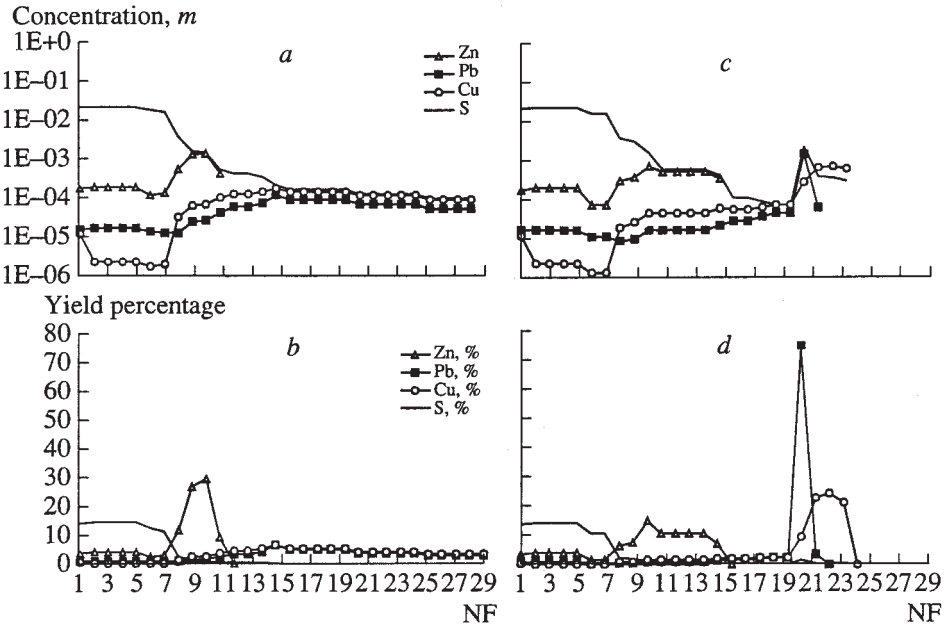

Fig. 60. Models of the mobilization of ore components at a temperature decrease in the reactor (the composition and pressure correspond to those in model IS-2). (*a, b*) The temperature decreases by 10°C over every five waves: 370, 360, 350, 340, 330, and 320°C; (*c, d*) the temperature decreases by 20–30°C over every five waves: 370, 350, 330, 310, 280, and 250°C.

common, while bornite, chalcocite, and other minerals are rare. Thus, the analysis of the models should reveal the conditions under which Cu leaching is suppressed or at least hampered.

The example of the basic model demonstrates that the sulfide sulfur concentration in pristine granite is 0.1–0.15 wt % (for example, in the V. Zgid granite) and can maintain the succession Zn ≫ Pb > Cu throughout the whole leaching process (or at least over quite a long time interval). At lower S concentrations, the succession is Zn ≫ Pb = Cu.

Variations in the temperature or the total original rock mass in the zone of the rock–water reaction does not result in any significant modifications of the leaching succession.

A pressure decrease strongly affects Pb and Cu separation (Zn is the first element leached in all models). For example, when the pressure decreases from 1 to 0.6 kbar, up to 40–45% of Cu is retained in the rock when all Pb is already completely extracted. Barometric determinations pertaining to deep-sitting mineralization [Laz'ko *et al.*, 1981] yield 0.9–1.2 kbar for the nascent mineral stage and a decrease to 0.8–0.7 kbar late in this stage. The pressure gradients determined by Laz'ko *et al.* [1981] in the vein bodies are 100–250 bar per 100 m updip. It follows that pressure can significantly vary during ore formation and the conditions selected for the models are consistent with natural observations. It is quite probable that pressure decreases not only in fracture-hosted vein structures but also in the mobilization zones. Charts of mineral stages at deposits of the Sadon group usually show both intra- and interstage tectonic motions (see, for example, [Lyakhov *et al.*, 1994]). It can be hypothesized that every pulse of tectonic activation interrupted the mobilization process and expanded the filtration pathways of the primary solutions, i.e., rejuvenated or expanded the area of mobilization needed for the resumption of the interrupted ore-forming process. Interludes between tectonic motions in the mobilization zone are marked by a gradual temperature and pressure decrease. If the process of leaching is interrupted before ore elements are completely extracted, the system under pressures of 0.6–0.8 kbar or with sulfide sulfur concentrations of 0.1–0.15 wt % should yield the required mobilization succession: Zn ≫ Pb > Cu.

The composition of the primary solution can also affect the metalliferous potential of the leaching solutions. Some aspects of this phenomenon were discussed above. It was established that an increase in the $NaHCO_3$ concentration modifies the mobilization succession of Pb and Cu: Zn > Cu > Pb. The solutions responsible for these changes seem to have been hardly probable at the deposits in question (these solutions create strongly alkaline environments and extremely high albite contents during reactions with granite).

7. Our calculations indicate that the sulfide sulfur concentration in the leaching solutions ranges from $n \times 10^{-2}$ to $n \times 10^{-3}$ *m*, i.e., over the interval quite common for hydrothermal solutions. High S concentrations in solutions arise when the primary solution reacts with granite bearing even relatively low S contents (<0.1 wt %). These data demonstrate that there is no need to call for

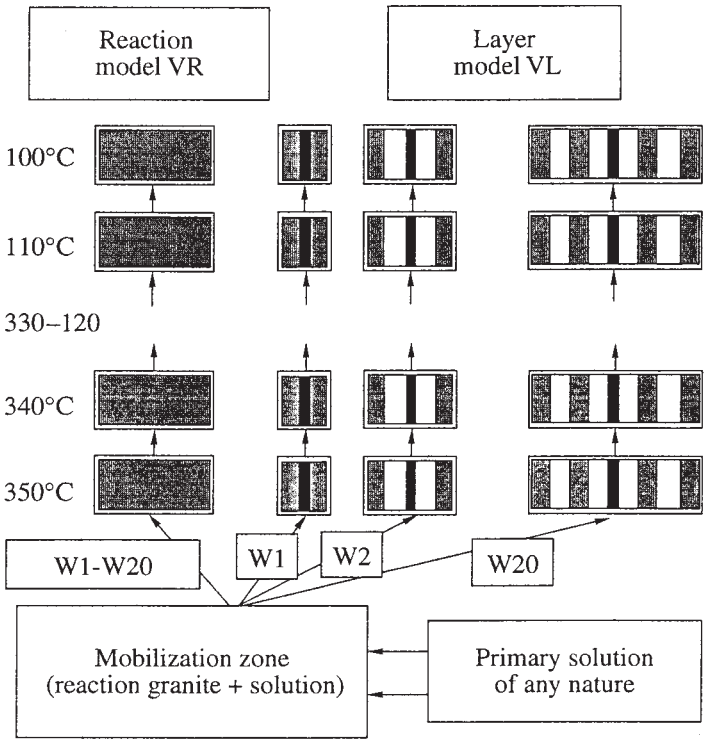

Fig. 61. Modeling scheme and model structures for the zone where filling veins are produced. W are waves of the solution from the mobilization zone, which are analogous to NF in Section 6.1.

any other source of S to maintain its high concentrations in the solution.

6.1.4. Conclusions

The equilibrium–dynamic modeling of the mobilization of ore components led us to establish the following:

(1) Interaction between primary barren solutions of any genesis and granites leads to the origin of metalliferous solutions, which can potentially be initial solutions for the hydrothermal system in question at elevated temperatures and pressures.

(2) Repeated interaction between barren hydrothermal fluids of constant composition with granites (at 310–420°C and 0.4–1.0 kbar) results in a significant increase in the concentrations of ore elements in the leaching solutions (up to $n \times 10^{-3}$ and $n \times 10^{-4}$ *m*) even without any changes in the external conditions.

(3) The metalliferous potential of the leaching solutions changes in the course of mobilization processes. Most of our models display the same unchanging leaching sequence of metals: the early stages of the process are dominated by the leaching of Zn, which is followed by Pb and Cu, i.e., Zn $\gg$ Pb $\geq$ Cu, and the solution becomes absolutely barren during the final stages of this process. A decrease in the pressure or sulfide sulfur content in the granite to 0.1–0.15 wt % partly impedes Cu extraction and results in the leaching succession Zn $\gg$ Pb > Cu.

(4) The concentration of S(II) in the leaching solutions ranges from $n \times 10^{-2}$ to $n \times 10^{-3}$ *m*, which fall within the range typical of medium-temperature hydrothermal deposits. These data demonstrate that there is no need to call upon other sources of sulfide sulfur for creating its realistic concentrations in the hydrothermal solution.

6.2. Model for the Genesis of Mineralized Veins

As was discussed above, the temperature gradients at our deposits can attain 20–40°C per 100 m updip the veins [Lyakhov *et al.*, 1978, 1994; Laz'ko *et al.*, 1981], and it can be hypothesized that a temperature decrease is one of the dominant factors of ore deposition. Proceeding from these facts and considerations, we model the changes in the equilibria in an ascending solution flow from the zone of metal mobilization in granite.

6.2.1. Simulation technique

The vein is modeled by a succession of 21–26 flow-through reactors (Fig. 61). Reactor 1 ("entrance" to the vein from below), into which the solution comes from the zone where metals are mobilized, has a temperature 20°C lower than the mobilization zone (350°C in most of our models, although we also analyzed other starting